JOURNAL OF SOLID STATE CHEMISTRY **127,** 137–144 (1996)
ARTICLE NO. 0369

The Computational Investigation of the Phase Transition from the GeO_2 α-Quartz Structure to the Rutile Structure

A. R. George and C. R. A. Catlow

Davy Faraday Research Laboratory, The Royal Institution, 21 Albemarle St., London, United Kingdom

Received November 6, 1995; in revised form August 7, 1996; accepted August 8, 1996

We report a detailed computational investigation using several techniques relating to the phase transition from the α-quartz to the rutile structure for GeO_2 and GeO_2/SiO_2 solid solutions. We calculate an activation barrier of approximately 47 kJ mol^{-1} for the phase transition, which is in good agreement with the most recently reported experimental value. We also identify a number of interesting intermediate structures, in which Ge is present in two coordination environments (fourfold and sixfold). These complex intermediates have characteristics akin to the experimentally observed amorphous systems. © 1996 Academic Press

INTRODUCTION

Naturally occurring GeO_2 is known to be more stable in the rutile (1) than in the α-quartz (2) structure, which is stable under ambient conditions for pure SiO_2, and the transition of GeO_2 between these phases has attracted much attention because of its similarity to the quartz–stishovite transition of SiO_2. The phase transition (3) has been studied under nonambient temperatures and pressures using *in situ* XRD techniques, and from energy dispersive diffraction data, recorded at several temperatures and pressures, an activation energy of 57.4 kJ mol^{-1} can be determined for the transition using the Avrami–Erofeev model for solid–solid transition (4). The transition has also been investigated using vibrational spectroscopy and a detailed investigation using IR, Raman, and XRD has been reported by Maddon *et al.* (5). An important feature of their work is the demonstration of the existence of an intermediate amorphous GeO_2 phase.

Periodic electronic structure calculations have been used to calculate the energy differences of the structures as a function of applied pressure (6) and the results were found to be in good agreement with experimental data. In the present paper, we apply both static and dynamic simulations based on interatomic potentials in order to study the detailed mechanism of the transition. These methods have the advantage of being computationally far cheaper than electronic structure techniques, thereby allowing both larger unit cells and a larger number of configurations to be examined. In a previous study (7), we applied these techniques to the structures and stabilities of mixed Si/Ge and pure end member Ge analogs of microporous silicate systems (8, 9). The present paper concentrates on the two dense phases, quartz and rutile. We exploit the ability of current computational techniques to perform calculations on large supercells (10) in order to derive atomistic models for the transition between the two phases. The success of our approach is shown by our calculation of an activation barrier that is in good agreement with the experimental value.

METHODOLOGY

The methodology and computational techniques, as well as the potential model used in this investigation, have been reported previously (7). Lattice energy minimization calculations were performed on each system, using shell model potentials (11) which describe polarization effects simply and reliably. Potentials for alumino-silicates are readily available (12) and details are given in the Appendix. The parameters for the Ge–O interaction were developed using an empirical fitting procedure by Bell (13). The lattice energy calculations employ the now standard summation procedures for the short range and Coulombic interactions, with the latter evaluated using the Ewald (14) technique. Full energy minimization may be undertaken with respect to both cell dimensions and atomic coordinates and the THBREL (15) code was used for all the lattice simulations; it embodies the summation procedures summarized above, coupled with a Newton–Raphson minimization (16) method.

The generation of the predicted infrared spectra is performed using the relaxed structure and the corresponding interatomic potentials. We employ standard lattice dynamical theory based on the harmonic approximation (which has been extensively applied to silicates by Parker and Price (17)). The calculations use the THBPHON (18) code,

0022-4596/96 $18.00
Copyright © 1996 by Academic Press
All rights of reproduction in any form reserved.

which generates both the frequencies and the atomic displacement vectors of the vibrational modes by diagonalizing the dynamical matrix of the system, without any use of the symmetry properties. The infrared (IR) and Raman spectra can be derived from the vibrational frequencies, by dividing the modes into infrared active, Raman active, and inactive modes using group theoretical projection methods (19). The position of the spectroscopic lines can then be calculated, while the IR line intensities are evaluated using the method of Kleinman and Spitzer (20). As argued in reference (21), the spectrum obtained can be made more directly comparable with experiment, by fitting a Gaussian curve (22), with a half-width of 10 cm^{-1}, to each peak.

In a single unit cell of α-quartz, there are only a limited number of tetrahedral sites which are available for substitution and, indeed, the constraints imposed by such a small unit cell and the use of periodic boundary conditions could impose the α-quartz polymorph, which would be unable within these structural constraints to transform to another polymorph. In the present work, the number of unit cells of the α-quartz type structure is increased to a $2 \times 2 \times 2$ supercell and finally to a $4 \times 4 \times 4$ supercell in order to provide more internal degrees of freedom. The phase transition may then be modeled via standard computational procedures provided the procedure used allows the activation barrier to be surmounted.

In addition to the static modeling of the structure, a preliminary study of the dynamics of the system was undertaken via Molecular Dynamics (MD) (23). The theory of the MD theory has been extensively reviewed, for example by Gupa (24) and by Allen and Tildesley (25), so only the details of the ensemble and simulation box will be reported here. An NPT ensemble (constant pressure, constant temperature, and constant number of particles) was employed, with the initial ion positions being derived from the results of the constant pressure lattice energy minimization on the supercell of GeO_2. To increase the number of internal degrees of freedom, this cell was replicated to an independent $2 \times 2 \times 2$ supercell; thus 64 unit cells of the α-quartz structure are included in the simulation box, in which there are 588 independent atoms, comprising 192 germanium ions and 384 oxygen ions. A Boltzmann distribution of velocities was assigned to the atoms in accordance with a thermal energy of 300 K. The system was allowed to evolve over 50 ps; numerical integration was performed over an integral time step of 1 fs; structural data were collected over a period of 5 ps. The length of this simulation is sufficient, because the purpose of our MD calculation is to access the dynamical stability of the structure and not to calculate quantities such as diffusion coefficients, for which longer simulation runs would be required (25, 26). The amplitudes of the framework vibrations are reflected in the radial distribution functions (RDFs).

The code FUNGUS (27) was used to perform the simulations as it embodies all the desired features required for this study. It uses the Verlet Leap Frog algorithm (28) in order to perform the numerical integration over time; an Ewald summation is employed for the summation of the long-range Coulombic interactions. Once the MD simulation had been completed, lattice energy minimization was performed on the resulting structure.

In the subsequent investigation of the phase transition, the newly derived MD structure was further subjected to lattice energy minimization with the unit cell angles being varied in a systematic manner. In these calculations the hexagonal unit cell, $\alpha = \beta = 90°$, $\gamma = 120°$ is gradually changed by decreasing γ by increments of $\sim 5°$ and performing a minimization after each change; during each of these minimizations γ is held constant, with all other variables including the cell dimensions a, b, c, α and β being allowed to vary. Such a process was continued until $\gamma \approx 90°$, after which a standard, constant pressure minimization calculation was performed, in which both the cell parameters and the internal coordinates were relaxed to equilibrium. The results allow us to chart the transition from hexagonal structure to one with orthogonal cell axes.

RESULTS AND DISCUSSION

(*1*) *"Static" Calculations Relating to Solid Solutions of GeO_2/SiO_2*

As in our previous study, we report calculations both for the pure end member GeO_2 and for Si/Ge solid solutions. In the latter case, the structures simulated are based on random arrangements of Ge ions over the T sites. Figures 1a–1c show the change in the lattice cell parameter as a function of the mole fraction of Ge substituted into the supercell of α-quartz. The a cell parameter (Fig. 1a) is calculated to expand to a greater extent with Ge content than observed in the previously reported calculations (which were based only on a single unit cell), but a marked *decrease* in this parameter is calculated on going from 50 to 66% Ge. The b lattice parameter (Fig. 1b) shows a steady increase with mole fraction, as expected by Vegard's Law. However, the predicted change in the c lattice parameter with mole fraction is very different from that observed in any of the previously studied (7) structures. For structures with mole fractions up to 50% Ge, the lattice parameter increases, in line with the previous work (7); but at 50–66% Ge, there is a reduction of 17% in the magnitude of the c lattice parameter.

The explanation of this unusual behavior is best given by reference to the energy minimized structures shown in Figs. 2a and 2b, which show, respectively, a view down the c axis, [001], and an orientation viewed along the b axis, [010]. Clearly, there is a structural change when 50 to 66% mole fraction of Ge is substituted into SiO_2, and it is this

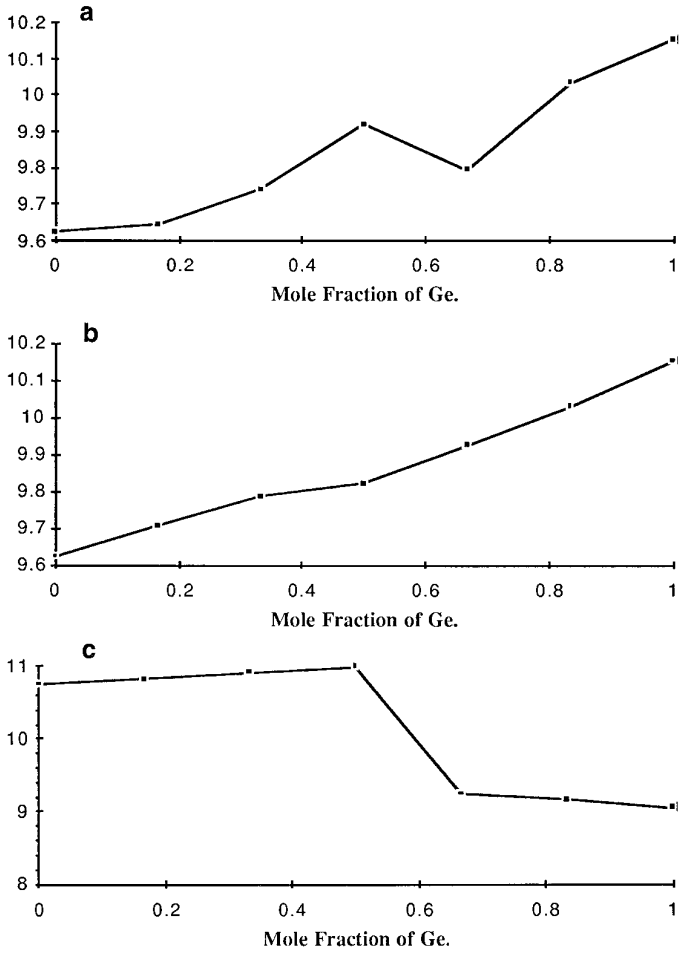

FIG. 1. The variation in the calculated lattice parameter as a function of the mole fraction of Ge substituted into the α-quartz supercell structure. (All lattice parameters in Å.)

change that is responsible for the substantial change in the *c* lattice parameter (Fig. 1c). In this context we note that the apparent increase in the intensity of the lines drawn in Fig. 2 is due to the near superposition of bonds in neighboring layers; hence, the thinner the line, the better the overlap of the bonds along the axis being viewed. Our simulations predict a structural phase transition which depends on the Ge : Si ratio. The new computationally derived structure has an open pore type topology with channel dimensions of 4.85 to 5.10 Å.

Examination of the structure, a stereoscopic view of which is shown in Fig. 3, shows that some Ge atoms have increased their coordination number from 4 to 6, which again indicates that there has been a substantial change in the structure. This change to a mixed coordination environment for Ge has been observed experimentally in a number of studies (29, 30). In the α-quartz structure, all the T atoms are 4 coordinate, in contrast to the rutile structure which is based entirely on octahedral coordination. The mixed coordination, and cooresponding mixed bond lengths, suggests that this structure and the others calculated could be plausible intermediates in the phase change from α-quartz to rutile as the mole fraction of Ge increases.

The energy of the new pure GeO_2 structure (−123.56 eV per T site) is more negative than that for the pure GeO_2 α-quartz structure by 31.84 kJ/mol per T site, although the pure GeO_2 rutile polymorph has an energy which is 82.98 kJ/mol lower per T site. Thus the calculated energies also suggest that the new structure is a possible intermediate in the structural phase transition from α-quartz to rutile. This partial change to the rutile structure is also evident in the *a*/*c* ratio; the value of this ratio for the intermediate calculated structure found by lattice energy minimzation is 1.12, between that of quartz (0.89) and of rutile (1.39).

As discussed earlier, we can calculate the IR spectra of the solids using procedures based on the quasi-harmonic approximation. We can also straightforwardly calculate the XRD spectrum since the atomic fractional coordinates and cell parameters are known. Thus, Fig. 4 shows the predicted IR spectra while Fig. 5 reports the XRD pattern during the gradual substitution of Ge into the supercell of the α-quartz structure. The phase change is clearly manifested by these results. The calculated IR spectrum for the pure α-quartz phase of GeO_2 is in agreement with the previously reported experimental data in that it clearly possesses three different groups of vibrational modes which are observed in all experimental studies (5). Moreover, the predicted IR spectrum of the new GeO_2 structure shows a major peak at around 925 cm^{-1}, a secondary peak at 810 cm^{-1}, and two groups of more complex lattice vibrations at lower wavenumbers. It is interesting to note that such peak patterns are in agreement with the experimental IR spectra of the amorphous GeO_2 as reported by Maddon *et al.* (5) and the references contained therein. It is plausible to suggest that the models we have developed by our simulations may be the closest representations possible to such an amorphous phase, given the constraints imposed by our cell size and the use of periodic boundary conditions.

(2) *Dynamical Calculations Relating to the Novel GeO_2 Structure*

A constant pressure and temperature (NPT) molecular dynamics simulation was performed on the intermediate structure located via lattice energy minimization (Fig. 3). After an initial equilibration period of 50 ps, data acquisition was carried out over a 5 ps time period. Figures 6a and 6b show a snapshot of one of the conformations sampled by the MD simulation, with, respectively, a view aligned along the [001] and the [010] cell axis. The structure is different from that produced by the energy minimization procedure (Fig. 3). The hexagonal nature of the cell is clearly retained even though the MD simulation was performed under con-

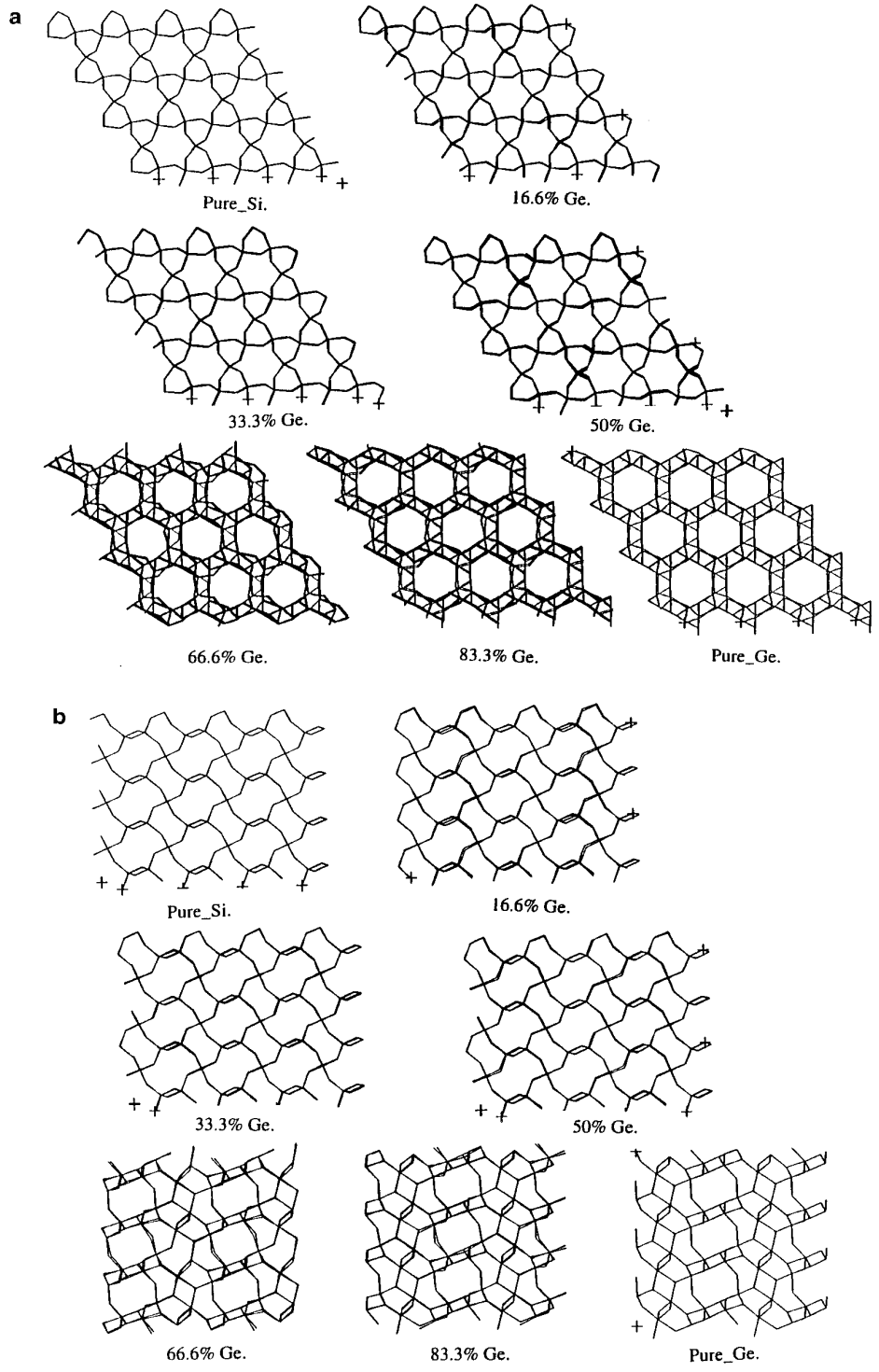

FIG. 2. (a) The resulting geometry optimized structures obtained on substituting Ge into an α-quartz structure viewed along [001]. (b) The intermediate structures viewed along [010].

stant pressure. The pores of the new structure are more clearly defined (especially when viewed along the [001]) (Fig. 6a) than those identified in the initial energy minimized structure and indeed they have increased in size to 5.17 Å. (We note this value is the internuclear distance and does not include the effective van der Waals radii which will make the actual noncontact pore dimensions smaller.) However, when viewed along the [010] there is

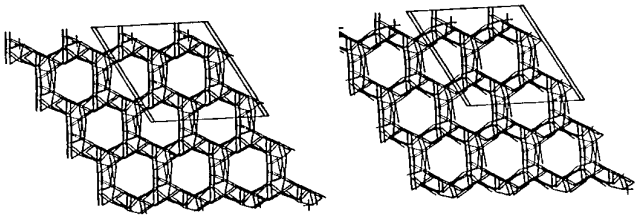

FIG. 3. A stereoscopic view of the new pure GeO_2 structure.

an increased connectivity (two ions are said to be connected when the distance is within the sum of the ionic radii of the two species). The average coordination number of the T sites has increased compared to that of the initial structure. This can clearly be seen by a comparison of the connectivity when viewed along the [010], both before and after MD (Figs. 2b and 6b, respectively). There is no evidence of any further phase change following that reported in the previous section and the structure derived after lattice energy minimization and a subsequent MD simulation bears *no* resemblance to the initial α-quartz structure. Indeed, energy minimization of the MD located structure yields an energy of -123.83 eV per T site which is lower than the starting structure (-123.56 eV per T site) although the rutile structure is still more stable. Evidently there is an energy barrier between the initial structure and the final structure located by the MD simulations. However, the magnitude of such a barrier must be small since it can be surmounted by performing a simulation at 300 K.

The MD simulation also provides information regarding the behavior of the structure over a time averaged period at the defined temperature. Figures 7a–7c report the normalized RDFs obtained from the MD simulation of the newly derived GeO_2 structure; they include O–Ge, O–O, and Ge–Ge pair correlations. In the O–Ge RDF shown in Fig. 7a there are evidently two different types of O–Ge bonds as shown by the two peaks in the RDF, centered on 1.77 and 2.03 Å, respectively. Clearly, the first peak at 1.77 Å is more intense than the second by a factor of approximately 3 (as can be verified by integration of the peaks). Thus approximately 75% of Ge–O bonds are at a distance of 1.77 Å, with the remainder about 2.03 Å in length. This observation discriminates between the oxygen atoms involved in tetrahedral and octahedral coordination; in the α-quartz structure, which is of course purely tetrahedrally bonded, only one O–Ge bond distance would be expected. Once again it is clear that we have a structure which is intermediate in the phase transition from α-quartz to rutile.

(*3*) *Calculation in which the Cell Angles are Varied*

All the calculations considered so far have involved constant pressure simulations, in which the unit cell parameters, both dimensions and cell angles, have been allowed to change. Clearly, there is a large activation barrier for the transition from the α-quartz to the rutile structure. The work described in this section uses the structure derived from the MD simulation, which we recall has an energy that is intermediate between the two stable polymorphs, and directly changes the unit cell angles (as discussed in the Methodology) by decreasing the cell angle by 5° and performing lattice energy minimization while keeping all the cell angles fixed and performing a subsequent minimization to locate the nearest local minima. Once the cell angle has been reduced to a value of 90°, a standard constant pressure minimization is undertaken allowing cell

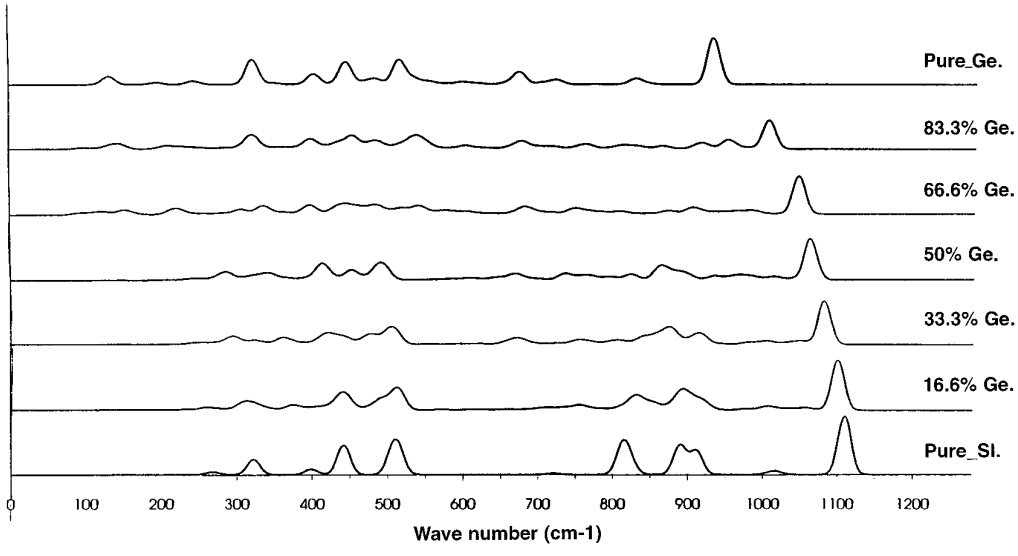

FIG. 4. The computed IR spectrum for the substitution of Ge into α-quartz to yield the new structure. (Intensity in arbitrary units.)

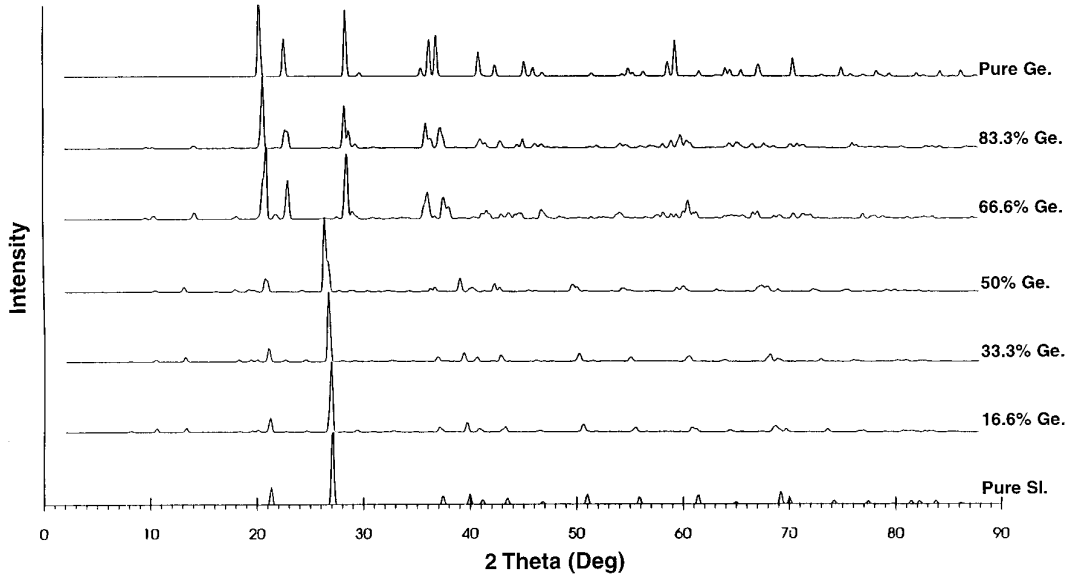

FIG. 5. The computed XRD pattern for the substitution of Ge into the α-quartz structure. (Intensity in arbitrary units.)

angles, dimensions, and internal coordinates to change freely; this final minimization has been termed ''unconstrained'' for future reference.

Figure 8 reports the variation in energy of the subsequent structures and also the final energy of the unconstrained minimization and that calculated for the rutile structure. We note that there is initially an increase in the energy per T atom as the cell angle γ is reduced; yet on going from $\gamma = 105°$ to $\gamma = 100°$, a substantial decrease in energy is calculated; upon continued decrease of the γ cell angle, a second activation barrier has been identified in the possible progression of the ''MD structure'' to the rutile structure. Indeed, such a result is not surprising considering the multidimensional energy surface and the large number of local minima which would be expected. Indeed, such local minima could be approximate models for ''amorphous'' phases. From this study, we are able to calculate the largest activation barrier of +0.48 eV (47 kJ mol^{-1}) for the quartz/rutile transition. This calculated barrier is in good agreement with the recently reported (4) experimental activation barrier calculated by the Avrami–Erofeev equation for the solid–solid transition which we recall is 57.4 kJ mol^{-1}. However, larger activation barriers of 83.7 kJ mol^{-1} (31) and 121.8 kJ mol^{-1} (32) were reported in earlier work; the discrepancies have been attributed to the effects of nucleation and growth rates and the grain size of the samples. We should stress that barriers of this magnitude could not be simulated directly by MD techniques. With static lattice modeling we are, however, able to study the high energy saddle points between the two phases.

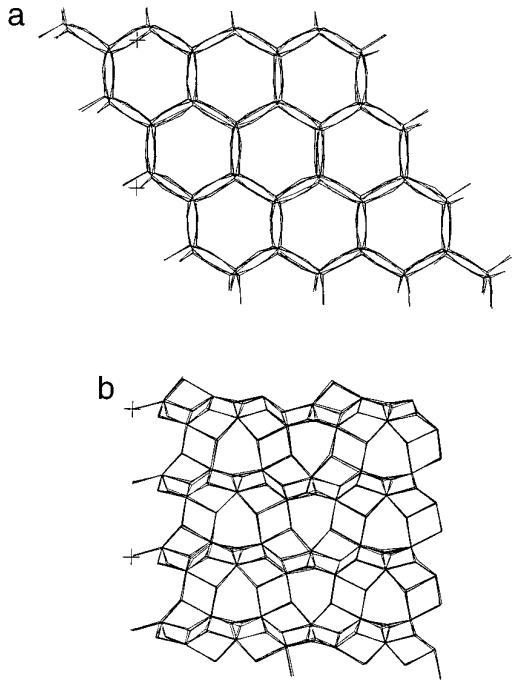

FIG. 6. A snapshot of one conformation sampled in the MD simulation; viewed along both the (a) [001] and (b) [010] cell axes.

In summary, the phase transition of pure GeO_2 from the α-quartz type structure to the rutile structure has been successfully modeled and we have identified a saddle point for the activated transition. This saddle point contains Ge ions in either fourfold or sixfold coordination environments which is in agreement with the available experimental data (5).

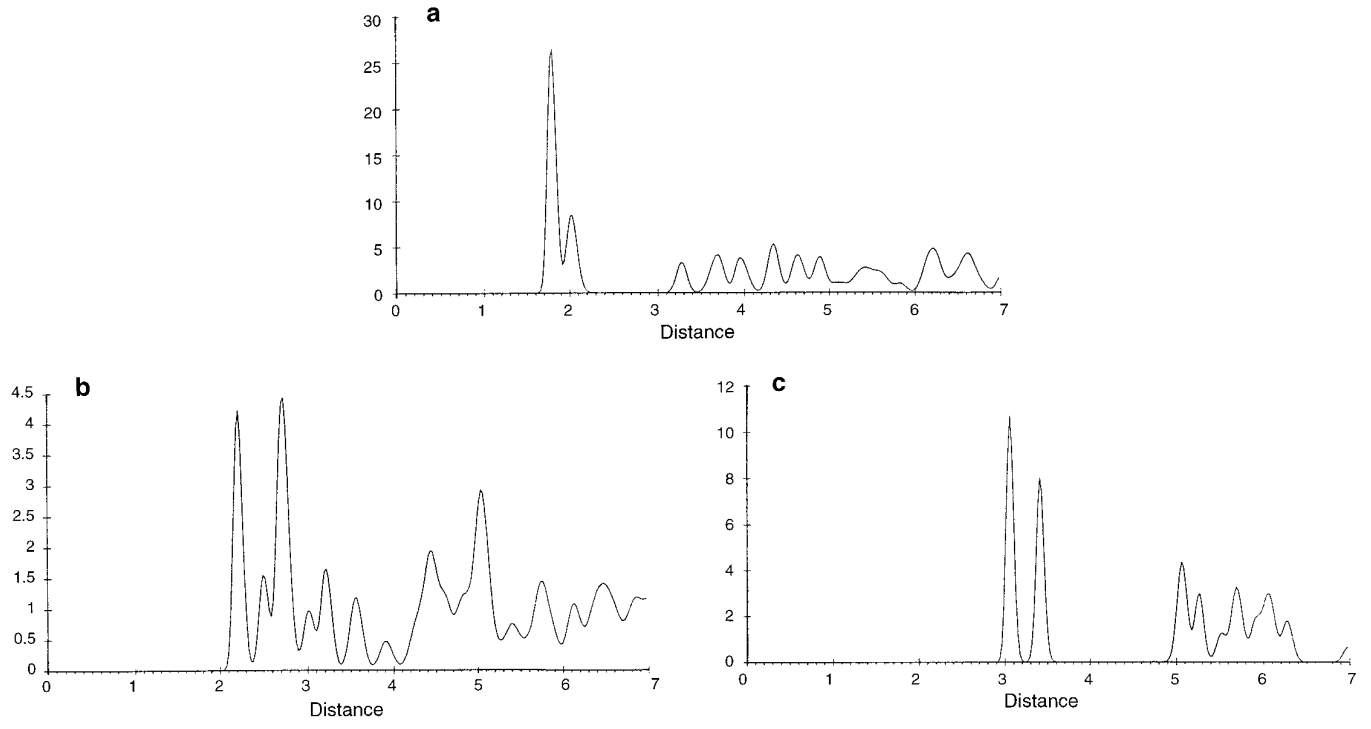

FIG. 7. The calculated radial distribution functions for the new GeO_2 structure; (a) O–Ge, (b) O–O, and (c) Ge–Ge. (The intensity is measured in arbitrary units and the distance is in Å.)

CONCLUSIONS

The work reported in this paper has allowed us to develop detailed models for the phase transition of the GeO_2-quartz structure; and key intermediates have been proposed for the transition. The calculated activation barrier of 47 kJ mol^{-1} is in good agreement with the experimental solid–solid activation barrier. The structures of a number of intermediates have also been proposed in which two coordination environments (fourfold and sixfold) exist. These structures could be considered as simple models for the experimentally observed amorphous phase.

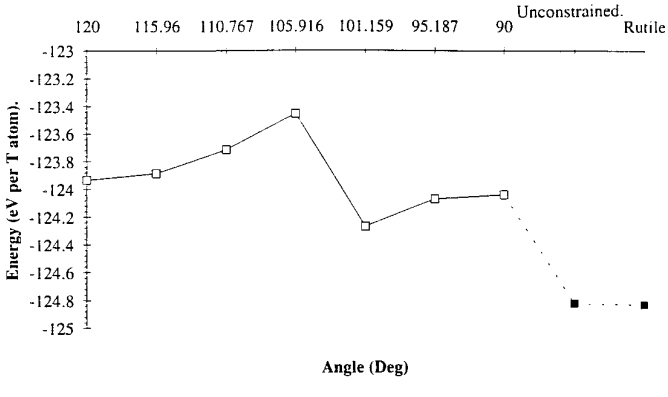

FIG. 8. The variation in the calculated energy per T atom as a function of the γ cell angle reduction.

APPENDIX: THE POTENTIALS USED IN THIS STUDY

Atomic parameters	Core charge (|e|)	Shell charge (|e|)	Spring constant (eV/Å^2)
Silicon	4.000	—	—
Germanium	4.000	—	—
Oxygen	0.869	−2.869	74.92

Interatomic Buckingham potential terms: $V_{ij} = A_{ij} \exp\left(-\frac{r_{ij}}{\rho_{ij}}\right) - \frac{c_{ij}}{r_{ij}^6}$.

Interaction	A (eV)	ρ (Å)	c_{ij} (eVÅ^6)
Silicon–oxygen (shell)	1283.9	0.3205	10.7
Germanium–oxygen (shell)	1980.0	0.3172	53.7
Oxygen (shell)–oxygen (shell)	22764.0	0.1490	27.9

Three-body terms: Energy $= k_{ijl}[\varphi_{ijl} - \varphi^o_{ijl}]^2$.

O–Si–O	$k_{ijl} = 2.10$ eV rad^{-2}	$\varphi^o_{ijl} = 109.47^o$
O–Ge–O	$k_{ijl} = 0.59$ eV rad^{-2}	$\varphi^o_{ijl} = 109.47^o$

ACKNOWLEDGMENTS

EPSRC are thanked for the provision of computing facilities and we are grateful to BIOSYM Technologies for supplying the InsightII software used in the graphical representations of structures. We are grateful to Prof. Sir J. M. Thomas for useful discussions.

REFERENCES

1. V. G. Hill, and L. L. Y. Chang, *Am. Mineral.* **53,** 1744 (1968).
2. B. Houser, N. Alderding, R. Ingalls, and E. D. Crozier, *Phys. Rev. B.* **11,** 6513 (1988).
3. V. G. Hill, and L. Y. C. Luke, *Am. Mineral.* **53,** 1744 (1968).
4. T. Yamanaka, K. Sugiyama, and K. Ogata, *J. Appl. Crystallogr.* **25,** 11 (1992).
5. M. Maddon, Ph. Gilet, Ch. Julien, and G. D. Price, *Phys. Chem. Miner.* **18,** 7 (1991).
6. L. H. Jolly, B. Silvi, and P. Darco, *Eur. J. Miner.* **6,** 7 (1994).
7. A. R. George, C. R. A. Catlow, and J. M. Thomas, *J. Solid State Chem.* **104,** (1993).
8. R. H. Jones, J. Chen, J. M. Thomas, A. R. George, M. Hursthouse, R. Xu, S. Li, Y. Lu, and G. Yang, *Materials* **4,** 808 (1992).
9. M. H. Tuilier, A. Lopez, J. L. Guth, and H. Kessler, *Zeolites* **11,** 662 (1991).
10. R. A. Jackson, J. E. Huntingdon, and R. G. J. Ball, *J. Mater. Chem.* **47,** 6777 (1991).
11. C. R. A. Catlow, and W. C. Mackrodt (Eds.), ''Computer Simulation of Solids,'' Lecture Notes in Physics, Vol. 166, Springer-Verlag, Berlin/New York, 1989.
12. R. A. Jackson, and C. R. A. Catlow, *Molec. Sim.* **1,** 207 (1988).
13. R. G. Bell, private communication.
14. P. P. Ewald, *Ann Phys. Leipzig,* **64,** 253 (1921).
15. M. Leslie, Daresbury Laboratory technical memorandum, in preparation.
16. R. Fletcher, ''Pratical Methods of Optimisation, Volume 1.'' Wiley, New York, 1980.
17. S. Parker, and D. Price, *in* ''Advances in Solid State Chemistry'' (C. R. A. Catlow, Ed.), Vol. 1, p. 295, 1989.
18. S. Dolling, *in* ''Methods in Computational Physics'' (G. Gilet, Ed.), Vol. 15, 1976.
19. A. A. Maradudin, E. W. Montroll, G. H. Weiss, and I. P. Ipatova, ''Theory of Lattice Dynamics in the Harmonic Approximation Approach.'' Academic Press, New York, 1971.
20. D. A. Kleinman, and W. G. Spitzer, *Phys. Rev.* **125,** 16 (1962).
21. A. J. M. de Man, Ph.D. Thesis, Eindenhoven University, Holland, 1992.
22. A. Mieiznikowski, and J. Hanuja, *Zeolites* **7,** 249 (1987).
23. P. Demontis, and G. B. Suffritti, *in* ''Modelling of Structure and Reactivity in Zeolites'' (C. R. A. Catlow, Ed.). Academic Press, San Diego, 1992.
24. S. Gupa, *Comp. Phys. Comm.* **70,** 243 (1992).
25. M. P. Allen, and D. J. Tildesley, ''Computer Simulation of Liquids.'' Clarendon Press, Oxford, 1987.
26. E. H. Hernandez, Ph.D. Thesis, University College, London, 1993.
27. B. Vessal, M. Leslie, and C. R. A. Catlow, *Molecular Sim.* **3,** 123 (1989).
28. L. Verlet, *Phys. Rev.* **159,** 98 (1967).
29. D. J. Durben, and G. H. Wolf, *Phys. Rev. B.* **43,** 2355 (1991).
30. J. P. Itie, A. Polian, G. Calas, J. Petiau, A. Fontaine, and H. Tolentino, *Phys. Rev. Lett.* **63,** 398 (1989).
31. N. S. Brar, and H. H. Schloessin, *High Temp. High Press.* **13,** 313 (1981).
32. R. J. Zeto, and R. Roy, ''Proc. 6th Int. Symp. on the Reactivity of Solids, Schenecady, New York, 1968'' (J. W. Mitchell, R. C. DeVries, R. W. Roberts, and P. Cannon, Eds.), pp. 803, 1969.